



## *Calf thymus* DNA–metal ions interactions: Calorimetric and spectroscopic thermal studies

Hiléia K.S. Souza\*

Centro de Investigação em Química – CIQ(UP), Department of Chemistry, Faculty of Science, University of Porto, Rua do Campo Alegre, 687, P-4169-007, Porto, Portugal

### ARTICLE INFO

#### Article history:

Received 19 September 2009

Received in revised form

14 December 2009

Accepted 18 December 2009

Available online 28 December 2009

#### Keywords:

*Calf thymus* DNA

Metal ions and thermodynamic parameters

### ABSTRACT

Calorimetric and spectroscopic studies on the interaction of *Calf thymus* DNA with divalent metal ions have been carried out in order to investigate how different ionic strengths as well as different divalent cations affect the thermal stability of the DNA double helix. The thermodynamic parameters of thermal denaturation of ds-DNA have been determined from solutions containing  $Mn^{2+}$ ,  $Co^{2+}$ ,  $Ni^{2+}$ ,  $Cu^{2+}$ ,  $Zn^{2+}$  and  $Cd^{2+}$  ions in different concentrations. The results obtained indicated that the nature of the interactions of the metal ions with the DNA molecule depends on metals ion concentration. At low metal concentrations there are no significant changes in the melting temperature value. However at high metal concentrations a decrease in melting temperature was observed, showing that the presence of high divalent cation concentration decreases the double helix stability. Further, it is also shown that the cations tested have significantly different interactions with DNA, even at the same concentration. This reveals clearly that not only the ionic strength is important in DNA stability, but that the changes observed in stability and thermal profile depend largely on the metal used.

© 2009 Elsevier B.V. All rights reserved.

### 1. Introduction

Metal ions are ubiquitously distributed in the environment. Many of them, such as cobalt, nickel, zinc, calcium and iron, are essential components of biological systems. Usually, transition metals have a strong base pair-affinity. They can coordinate directly to the nucleophilic atoms of bases and, thus perturb the hydrogen bonding between base pairs, resulting in a destabilization of DNA. As such, the active biological role of metal ions, in particular their interaction with the DNA molecule [1–3], has been attracting increasingly the interest of many research groups.

The way metals interact with the DNA structure is very important from the point of view of nucleic acids biophysics and molecular biologists. Metal binding to DNA and its effect on the conformational state has been previously described in the literature [4]. In general, for Na-salt *Calf thymus* DNA, the multivalent cations electrostatically bind at the entrance of the B-DNA major groove (between the two phosphate strands) repelling the sodium counterions from the neighbouring phosphates which are strongly attracted to the groove-bound cation leading to groove closure and DNA bending [5].

The stability and conformation of DNA in the presence of metal ions have been previously studied by a variety of techniques such as fluorescence [6], circular dichroism [7,8], electron microscopy [9], FTIR [10], NMR spectroscopy [11] and others. The study of the conformational changes of nucleic acids has developed mainly due to two new factors: first, the improvement of biochemical preparation techniques of native DNA and DNA fragments and ability to manipulate native conformation or engineering new sequences; second, the use of highly sensitive experimental techniques (e.g. differential scanning microcalorimetry) for the determination of the energy parameters of the conformational transition. Micro-DSC has proved particularly suitable for the study of the conformational transitions of DNA double helix in dilute solution [12,13] surpassing the traditional use of other techniques such as UV spectroscopy [14,15] to determine the energetics of the transition, particularly because the calorimetric enthalpy can always be obtained as a “model-free” parameter, which does not hold for most other techniques used.

In this work the effect of the metal ion, and its concentration, on the stability of *Calf thymus* DNA was studied by, differential scanning calorimetry. In order to get further information of the melting profile under the studied conditions, a spectroscopic technique (UV) was also used. Most studies of metal ions–DNA interactions found in the literature have been carried out at high metal concentrations. However, in solutions of low ionic strength, the DNA conformation should be more sensitive to the solution conditions. For this reason, in the present work all the experiments have been carried out in buffer solutions (with constant ionic strength) containing also the metal ions under study in the form of chlorides.

\* Present address: REQUIMTE, Chemical Engineering Department, Faculty of Engineering, University of Porto, Rua Dr. Roberto Frias, 4200-465 Porto, Portugal. Tel.: +351 225081884; fax: +351 22 5081449.

E-mail addresses: [hsouza@fe.up.pt](mailto:hsouza@fe.up.pt), [hileiak@yahoo.com](mailto:hileiak@yahoo.com).

## 2. Experimental

### 2.1. Material and solutions

NaCl (Merck; 99.5%) and  $C_6H_5Na_2O_7 \cdot 2H_2O$  (Merck; 99%) together with *Calf thymus* DNA (Sigma) and the hydrated chloride salts of the studied divalent metals ( $Mn^{2+}$ ,  $Co^{2+}$ ,  $Ni^{2+}$ ,  $Cu^{2+}$ ,  $Zn^{2+}$  and  $Cd^{2+}$ ) were from Aldrich, analytical grade and have been used without further purifications.

Three stock solutions were prepared in Milli-Q water for the DSC experiments. A sodium citrate buffer solution (ssc; pH 8.35) containing sodium chloride ( $0.3 \text{ mol dm}^{-3}$ ) and sodium citrate ( $0.03 \text{ mol dm}^{-3}$ ). A DNA stock solution ( $2 \text{ mg cm}^{-3}$ ) was obtained dissolving the *Calf thymus* DNA in the desired volume of ssc (sodium chloride  $0.15 \text{ mol dm}^{-3}$  and sodium citrate  $0.015 \text{ mol dm}^{-3}$ ). Stock solution for each divalent metal ion ( $0.5 \text{ mol dm}^{-3}$ ) was prepared by dissolving the corresponding chloride salt in Milli-Q water. For the experiences in the absence of metals, a reference solution (without DNA) was obtained by simple dilution of the ssc solution and a DNA containing sample was prepared by dilution of the DNA stock solution (DNA  $1 \text{ mg cm}^{-3}$ , sodium chloride  $0.15 \text{ mol dm}^{-3}$  and sodium citrate  $0.015 \text{ mol dm}^{-3}$ ).

A reference and a sample metal containing solutions (metal ion concentration range between  $0.002$  and  $0.010 \text{ mol dm}^{-3}$  sodium chloride  $0.15 \text{ mol dm}^{-3}$  and sodium citrate  $0.015 \text{ mol dm}^{-3}$ ) were prepared by mixing the appropriate volume of the three stock solutions.

For UV absorbance measurements solutions with a concentration of DNA ( $0.05 \text{ mg cm}^{-3}$ ) and metal ion ( $1 \times 10^{-4}$ – $2.5 \times 10^{-3} \text{ mol dm}^{-3}$ ) were prepared by 20 times dilution of the solutions used in the DSC experiments.

The DNA concentration (expressed in base pairs) was determined spectrophotometrically at  $20^\circ\text{C}$  using an extinction coefficient [16–22]:  $\varepsilon_{260} = 13,200 \text{ mol}^{-1} \text{ dm}^3 \text{ cm}^{-1}$ . The ratio of UV absorbance obtained for these solutions, at 260 and 280 nm, was about 1.8–1.9, indicating that the DNA was sufficiently free from protein contamination [18,23–30].

### 2.2. Techniques

#### 2.2.1. Differential scanning calorimetry (DSC)

DSC experiments were run on a Micro-DSC III Setaram apparatus, which has been shown to be suitable for working with dilute solutions of biological macromolecules. DSC experiments were performed using a scan rate ( $\beta$ ) of  $1^\circ\text{C min}^{-1}$ , and the sample was scanned between  $20$  and  $110^\circ\text{C}$ . The measurements were performed in a measuring cell charged with a solution volume equal to  $0.8 \text{ cm}^3$ , against a reference cell charged with the same volume of buffer. Buffer–buffer runs were performed in the same conditions to be used as blank experiments.

The instrument software (SETSOFT, Setaram) was used to perform the blank correction and to obtain the calorimetric enthalpy ( $\Delta H_{\text{cal}}$ ) by integration of the corresponding peak areas (Eq. (1)). The final  $C_p$  versus  $T$  plots were obtained from the experimental corrected signal by dividing it by the scanning rate

$$\Delta H_{\text{cal}} = \int_{T_1}^{T_2} C_p dT \quad (1)$$

The calorimetric entropy was determined using Eq. (2)

$$\Delta S_{\text{cal}} = \int_{T_1}^{T_2} \frac{C_p}{T} dT \quad (2)$$

The melting temperature ( $T_m$ ) was determined as the midpoint of the melting transition and was also provided by the used software.

In order to check whether the transition followed a two state model, commonly used for DNA denaturation [31–33] we did also perform a van't Hoff analysis of the calorimetric curves.

The van't Hoff enthalpy, ( $\Delta H_{\text{VH}}/\text{J mol}^{-1}$ ) [31–38] was obtained from the relation:

$$\Delta H_{\text{VH}} = \frac{\sigma RT_m^2 C_{pT_m}}{\Delta H_{\text{cal}}} \quad (3)$$

where  $\sigma = 6$ , in our experimental conditions,  $R$  is ideal gas constant,  $C_{pT_m}$  heat capacity at  $T_m$  and  $\Delta H_{\text{cal}}$  calorimetric enthalpy.

The average number of base pairs [16,23,26–28,34,36] in a cooperative melting unit was calculated considering the ratio.

The ratio:

$$\frac{\Delta H_{\text{VH}}}{\Delta H_{\text{cal}}} \quad (4)$$

was used to assess the validity of the two state model.

#### 2.2.2. UV-vis spectroscopy

UV absorbance measurements were carried on an AGILENT 8453 UV-visible spectroscopic system equipped with a thermoelectrically controlled cell holder and quartz cell with a pathlength of  $1.0 \text{ cm}$ .

Absorbance versus temperature data profiles were recorded after every  $0.15^\circ\text{C}$  and it were obtained by plotting the absorbance measured at  $260 \text{ nm}$  with a heating rate of  $1^\circ\text{C min}^{-1}$ .

The fraction of melted base pairs,  $\theta$ , was calculated from the standard formula [24,39,40]:

$$\theta = \frac{A - A_L}{A_U - A_L} \quad (5)$$

where  $A$ ,  $A_L$  and  $A_U$  are sample absorbance, absorbance of the lower baseline, and the absorbance of the upper baseline respectively.

$T_m$  is defined as the temperature for which  $\theta$  was 0.5.

The hyperchomicity [18,30,41,42] of the samples was calculated using:

$$\%H_{260} = \frac{A_U - A_L}{A_L} \times 100 \quad (6)$$

## 3. Results and discussion

Figs. 1–4 show the calorimetric curves obtained by micro-DSC for the thermal denaturation process of *Calf thymus* DNA in the absence and presence of different divalent transition metal ions at different concentrations. Table 1 summarizes the thermodynamic parameters obtained from these experiments as explained in Section 2.

The melting profile obtained for the DNA in the absence of metals (Figs. 1 and 2), agrees with the previously reported by different authors [16,27,30,42,43]. The curves showed a broad band going from  $80$  to  $100^\circ\text{C}$  with a fine structure formed by three peaks of similar intensity (A–C in Fig. 1a) and a smaller one (D). According to the previous work [16,27,42] the lower intensity of peaks B and D can be associated to the use of different experimental condition such as the heating rate or the buffer.

At low metal ion concentration the transition curves do not show significant differences (Fig. 3) and retain the main characteristics showed by the DNA denaturation in the absence of metals.

As the metal ion concentration is increased, the destabilization of the ds-DNA is clearly evident for all studied systems by a decrease in the temperature of onset of the transition (Figs. 1 and 2). However, the DSC profile, i.e., the bands shift of the  $C_p$  versus  $T$  plots is different for each metal, indicating that the process of denaturation

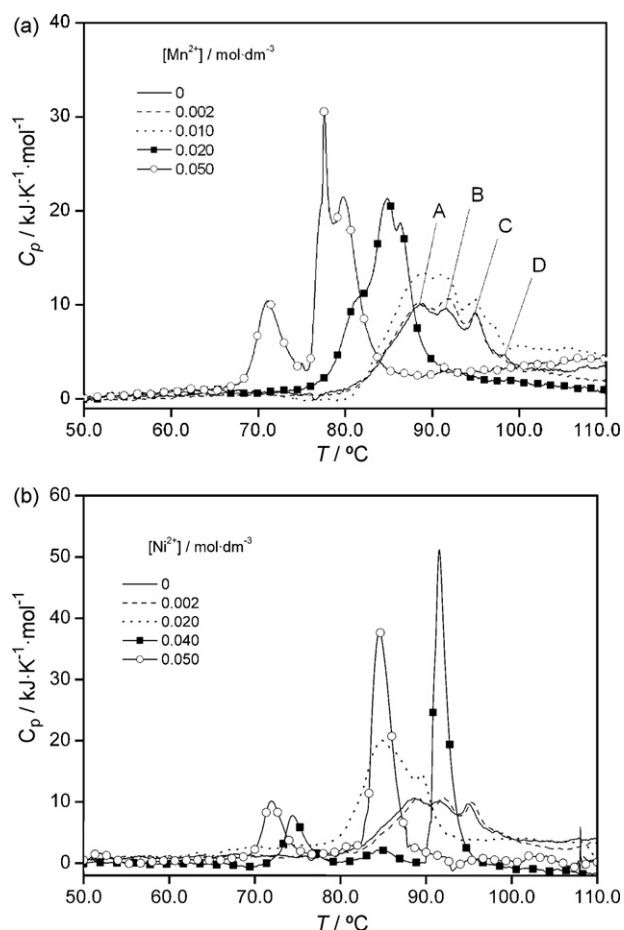


**Fig. 1.** Excess heat capacity as a function of temperature for ds-DNA solutions with different concentrations of  $\text{MnCl}_2$ . Citrate sodium buffer ( $[\text{NaCl}]$   $0.15$   $\text{mol}\cdot\text{dm}^{-3}$ ),  $[\text{DNA}]$   $1$   $\text{mg}\cdot\text{cm}^{-3}$ ,  $\beta = 1$   $\text{K}\cdot\text{min}^{-1}$ . (a)  $\text{MnCl}_2$  and (b)  $\text{NiCl}_2$ .

depends significantly on the concentration and the nature of these cations.

Fig. 4 shows the curves obtained at the highest metal ion concentration studied, i.e.,  $0.050$   $\text{mol}\cdot\text{dm}^{-3}$ . The profiles for  $\text{Cu}^{2+}$  and  $\text{Cd}^{2+}$  are not included due to their stronger interaction at such concentrations that leads to not well defined DSC profiles. In both cases, the formation of aggregates was observed by eye at concentrations higher than  $0.015$   $\text{mol}\cdot\text{dm}^{-3}$ . In general, the profiles present three peaks of higher intensity than the ones obtained for the denaturation of DNA in the absence of the metals (Fig. 4).  $\text{Mn}^{2+}$ ,  $\text{Co}^{2+}$  and  $\text{Ni}^{2+}$  present a first and small peak between  $70$  and  $75^\circ\text{C}$ . While in the case of  $\text{Mn}^{2+}$  and  $\text{Co}^{2+}$  this peak is followed by a more intense band around  $80^\circ\text{C}$  which is splitted into two peaks, in the case of  $\text{Ni}^{2+}$  we can see a second intense peak around  $85^\circ\text{C}$ . In the case of  $\text{Mn}^{2+}$ , a second peak appears between  $75$  and  $80^\circ\text{C}$  and a third (and less intense) peak around  $80^\circ\text{C}$ . For  $\text{Co}^{2+}$  this second peak was much more intense and narrow, and the third one showed the same intensity as the one for  $\text{Mn}^{2+}$ , becoming a shoulder in the peak. The presence of  $\text{Zn}^{2+}$ , however, led to a different calorimetric profile, especially at low temperatures. While the same splitted peaks appear at the same temperature than for  $\text{Mn}^{2+}$  and  $\text{Co}^{2+}$ , it showed two new and small peaks around  $60^\circ\text{C}$  and  $65$ – $75^\circ\text{C}$  respectively.

It is a well known fact that the energy necessary to melt GC pairs is higher than the one for AT, since the GC couples are bounded by three hydrogen bonds (versus the two needed for AT binding). This energy difference can be enhanced in the presence of agents with the ability of interact preferentially with the purine or the pyrimidine bases. This hypothesis has been proved in previous reports on the DNA stability in the presence of several destabilizing agents by different techniques [44–47]. Some of them suggested that the high temperature region of the calorimetric curves could be associated to the melting of the more energy demanding GC rich clusters [46,47]. The peaks corresponding to the low temperatures zone were then associated to the melting of AT pairs which requires less energy. It should be noted that previous studies [1–5,28,41,43,48,49] have suggested that these cations interact preferentially with GC pairs. This interaction usually involves N7

**Table 1**

Thermal denaturation parameters for *Calf thymus* DNA in the absence and presence of divalent metal ion. Citrate sodium buffer ( $[\text{NaCl}]$   $0.15$   $\text{mol}\cdot\text{dm}^{-3}$ ),  $[\text{DNA}]$   $1$   $\text{mg}\cdot\text{cm}^{-3}$ ,  $\beta = 1$   $\text{K}\cdot\text{min}^{-1}$ .

Sample	$c\text{ M}^{2+}/\text{mol}\cdot\text{dm}^{-3}$	$T_m/^\circ\text{C}$		$\Delta H_{\text{cal}}/\text{kJ}\cdot\text{mol}^{-1}$			$\Delta S_{\text{cal}}/\text{J}\cdot\text{K}^{-1}\cdot\text{mol}^{-1}$				$(\Delta H_{\text{VH}}/\Delta H_{\text{cal}})$				
							Total		Total						
DNA	0	90.4		89.1			89.1	257		257		8.8			
$\text{Mn}^{2+}$	0.002	90.5		99.5			99.5	286		286		6.3			
	0.010	89.8		115			115	337		337		5.9			
	0.020	84.7		128			128	353		353		7.3			
	0.050	71.1	79.1	31.2	104	135	80.6	273	354	62	11				
$\text{Co}^{2+}$	0.002	89.8		101			101	292		292		5.2			
	0.010	90.9		130			130	350		350		4.7			
	0.020	85.9		126			126	337		337		8.9			
	0.050	78.7		128			128	372		372		9.9			
$\text{Ni}^{2+}$	0.002	91.0		100			100	307		307		5.4			
	0.010	85.8		122			122	351		351		8.8			
	0.020	74.9	84.6	91.8	26.5	9.0	97.1	133	75.4	25.5	274	375	73	173	21
	0.050	72.1		84.8	30.4		110	140	79.4		297	376	91		23
$\text{Cu}^{2+}$	0.002	91.5		81.7			81.7	238		238		8.4			
	0.010	87.4		108			108	302		302		9.8			
	0.015	57.9	80.7	28.8	108	137	96.5	307	403	33	29				
$\text{Zn}^{2+}$	0.002	90.0		109			109	313		313		6.2			
	0.010	90.1		110			110	321		321		5.1			
	0.020	74.6	83.1	95.3	38.5	11.2	71.5	121	120	22.9	182	325	53	158	20
	0.050	60.3	66.9	80.4	28.2	13.6	84.2	126	77.1	30.7	233	341	98	282	17
$\text{Cd}^{2+}$	0.002	89.5		92.6			92.6	280		280		3.8			
	0.010	90.4		99.0			99.0	277		277		7.3			
	0.015	88.3		102			102	292		292		8.9			

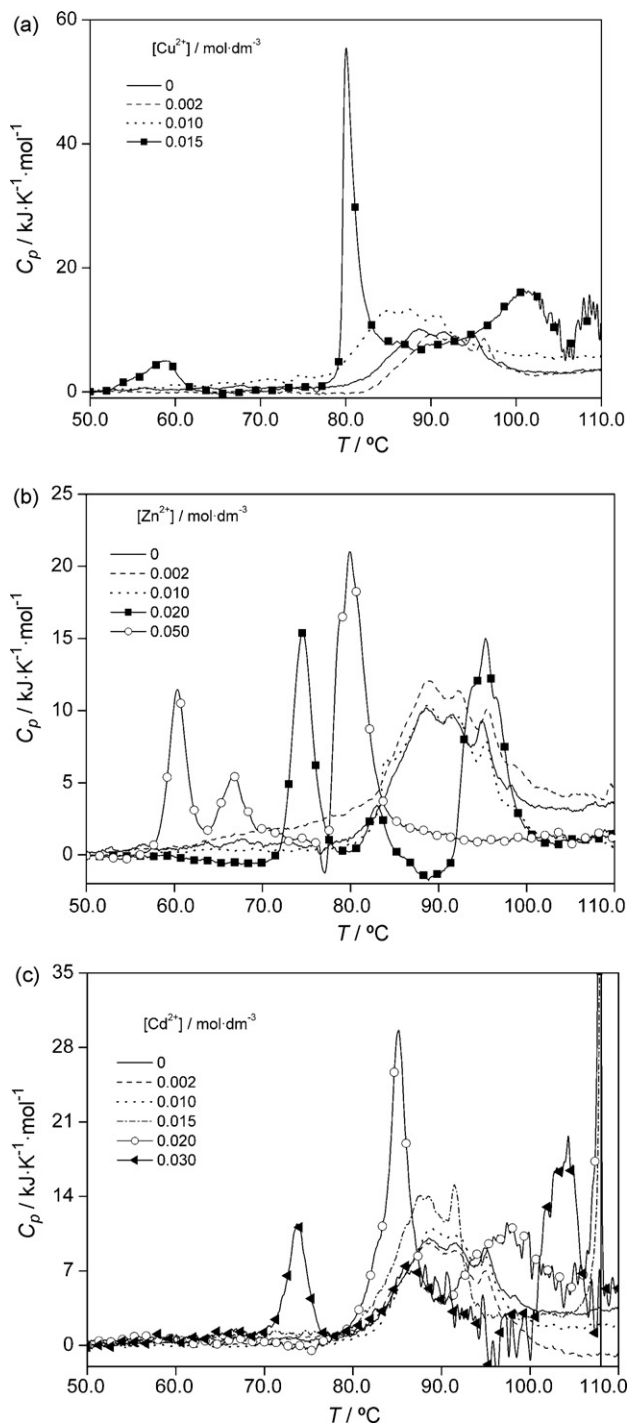


**Fig. 2.** Excess heat capacity as a function of temperature for ds-DNA solutions with different concentrations of  $MCl_2$ . Citrate sodium buffer ( $[NaCl] 0.15 \text{ mol dm}^{-3}$ ),  $[DNA] 1 \text{ mg cm}^{-3}$ ,  $\beta = 1 \text{ K min}^{-1}$ . (a)  $CuCl_2$ , (b)  $ZnCl_2$  and (c)  $CdCl_2$ .

and O6 of guanine, although cytosine O2 and N3 have been also considered for  $Cu^{2+}$ . These metals ions have been shown to interact preferentially by destabilizing the GC pairs. There are some evidences that they also interact, to a lower extent, with the AT moieties.

In some cases the metal ion can bind primarily to the phosphate, resulting in a stabilization of the DNA helix. The binding preference towards the base is usually higher than for the phosphates for these divalent metals, and the following order of preference has been established [3]:  $Cu^{2+} > Cd^{2+} > Zn^{2+} > Mn^{2+} > Ni^{2+} > Co^{2+}$ .

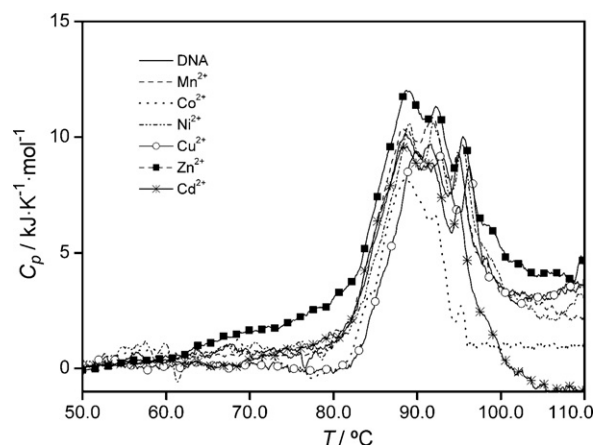


**Fig. 3.** Excess heat capacity as a function of temperature for ds-DNA solutions with different metal ions. Citrate sodium buffer ( $[NaCl] 0.15 \text{ mol dm}^{-3}$ ),  $[c] = 0.002 \text{ mol dm}^{-3}$ ,  $[DNA] 1 \text{ mg cm}^{-3}$ ,  $\beta = 1 \text{ K min}^{-1}$ .

The results presented in Fig. 4 can be analyzed in the scope of the interactions of the cations with GC and AT DNA base pairs. There is a group of metals that seems to interact with the AT bases in a similar way, namely:  $Mn^{2+}$ ,  $Co^{2+}$ ,  $Ni^{2+}$  and  $Cd^{2+}$ , if we consider the shape and position of the first peak.  $Zn^{2+}$  and  $Cu^{2+}$ , on the other hand, are the most destabilizing metals for DNA (decreasing the melting temperature to  $60^\circ\text{C}$ ) as a consequence of their stronger destabilization of the AT pairs. According to our calorimetric tracings,  $Zn^{2+}$  shows two peaks in the low temperature region, suggesting a different mechanism of interaction as compared to  $Cu^{2+}$ . Although the profiles at such high concentration were not obtained for  $Cu^{2+}$  and  $Cd^{2+}$ , the analysis of their curves at the highest concentration used suggested their inclusion in different groups. Focusing the analysis on the GC pair stability, we can perform a different grouping.  $Ni^{2+}$  and  $Cd^{2+}$  seem to disturb the stability of these pairs to a lower extent than a second group formed by  $Mn^{2+}$ ,  $Co^{2+}$ ,  $Zn^{2+}$  and  $Cu^{2+}$ . Thus, this difference could be associated to a different mechanism of interaction involving different base atoms. In that case the corresponding peak showed splitting. This behavior could be related to the melting of two kinds of GC–metal complexes of slightly different stability. The less stable (lower temperature) will correspond to simple GC–metal complexes while the second peak could be due to the fraction of complexes which are involved in phosphate chelation. The behavior of  $Zn^{2+}$  in the low temperature region could be also related to phosphate chelation of the AT metal complexes.

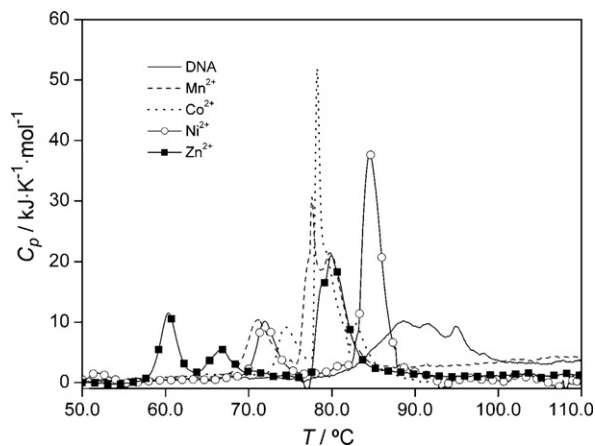


**Fig. 4.** Excess heat capacity as a function of temperature for ds-DNA solutions with different metal ions. Citrate sodium buffer ( $[NaCl] 0.15 \text{ mol dm}^{-3}$ ),  $[c] = 0.050 \text{ mol dm}^{-3}$ ,  $[DNA] 1 \text{ mg cm}^{-3}$ ,  $\beta = 1 \text{ K min}^{-1}$ .

The total calorimetric enthalpy increases with increasing of the metal ion concentration. Table 1 shows that the total calorimetric enthalpy at  $0.050 \text{ mol dm}^{-3}$  was around  $130\text{--}40 \text{ kJ mol}^{-1}$  for  $\text{Mn}^{2+}$ ,  $\text{Co}^{2+}$ ,  $\text{Ni}^{2+}$  and  $\text{Zn}^{2+}$ , suggesting that their interaction with DNA involves a similar energy, and therefore could be associated with similar processes. In the case of  $\text{Cu}^{2+}$  and  $\text{Cd}^{2+}$  the calorimetric enthalpies are missing in the table as at these concentrations the curves were not integrated (as explained above). This difference in behavior can be explained because these metal ions have an important and peculiar effect in the ds-DNA stability and structure, interacting with different groups in different sites of the macromolecule, influencing the structures canonic of the DNA.

Table 1 also shows that the total entropy increases with the increase of the metal ion concentration. This entropy increase can be also attributed to an increase in hydration water release in the thermal denaturation process due to the electrostatic interactions between the metal ion and the macromolecule. For  $\text{Zn}^{2+}$ , the total entropy did not change significantly with the increase in metal ion concentration.

The cooperativity of the transition is a very important question, and that lead to the calculation of the van't Hoff enthalpy from the calorimetric results, to try to assess it quantitatively. The ratio between the calorimetry enthalpy and van't Hoff enthalpy gives quantitative information on the cooperativity of the transition, that can also be qualitatively derived from the width of the denaturation profile. For the system studied here there was a significant difference between the calorimetric and the van't Hoff enthalpies (Table 1).

A ratio ( $\Delta H_{VH}/\Delta H_{cal} > 1$ ) is related with the mean number of nucleotides that melt as a single thermodynamic entity and may indicate significantly populated intermediate states [16,27,34,50]. It is an index of the mean cooperative unit size (in case of cooperative transition), as previously reported [16]. In this work, when the profiles present the main characteristics as those obtained for the denaturation of the DNA in the absence of metals, this ratio is lower as compared to the one obtained for the DNA alone. At high metal ion concentration, there is a shift in the shape of the profiles and the ratio increases as compared to DNA alone. These differences point to a change in the denaturation process due to the presence of the metal ions.

The effect on the transition width of the first addition of metal ion and the reduction in width with further addition is in agreement with other results in the literature [27]. This may be explained by considering the hypothesis that polyvalent cations are almost completely bounded to the double helix at low concentration. The stability of the "unmelted" regions increases, and the transitions are broadened, as a result of the partial denaturation of a helix that releases some cations, which are free to bind elsewhere on the same helix or on another one [27].

To increase the time which the DNA remained in the unfolded form, a decrease of the scan rate to ( $0.2, 0.5 \text{ K min}^{-1}$ ) have been done. The results do not show significant differences in the thermodynamic parameters values when compared with the results obtained at  $1 \text{ K min}^{-1}$ . In all cases the denaturation *calif thymus* DNA processes was irreversible.

In order to obtain information on the denaturation profile, the denaturation was also followed by UV. UV spectra were measured at  $260 \text{ nm}$  as a function of temperature for *Calif thymus* DNA in the absence and presence of divalent metal ion. The UV absorbing properties of the DNA arises from the  $\pi\text{--}\pi^*$  electronic transition occurring in the nucleotide bases. The changes in their electron density distribution as a consequence of the double helical stacking is reflected in the increase of the absorbance as it denatures [39].

The interaction between the metal ions and the DNA is known to depend on both the nature and the concentration of the metal ions [6,51,52]. Figs. 5–7 shows a significant change of the melting tem-

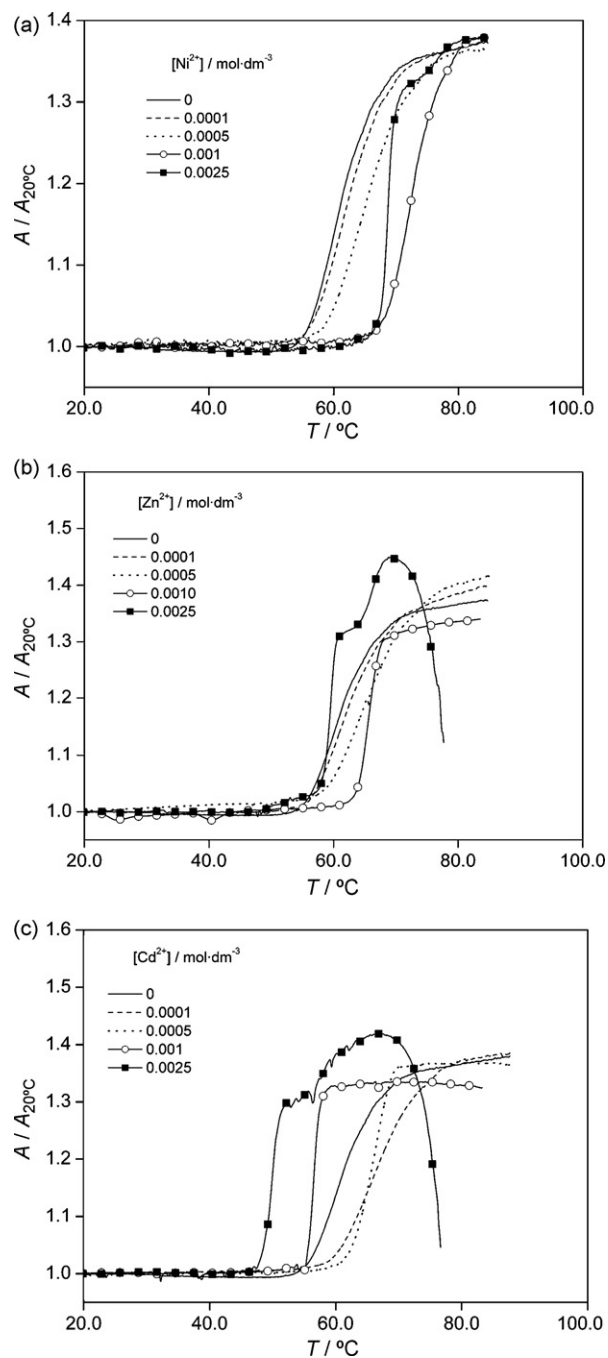
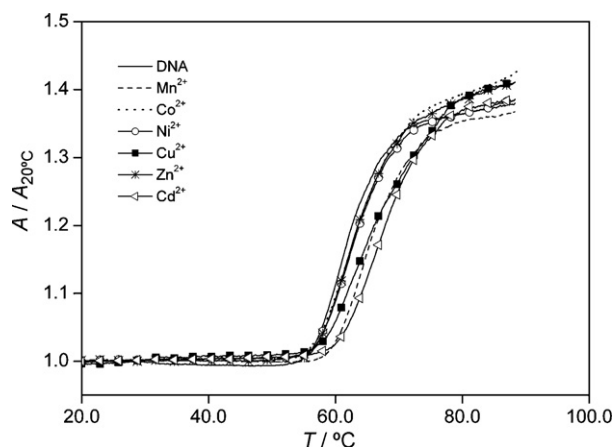


Fig. 5. Relative absorbance at  $260 \text{ nm}$  as a function of temperature for ds-DNA solutions with different concentrations of  $\text{MCl}_2$ . Citrate sodium buffer ( $[\text{NaCl}] = 7.5 \times 10^{-3} \text{ mol dm}^{-3}$ ),  $[\text{DNA}] = 0.05 \text{ mg cm}^{-3}$ ,  $\beta = 1 \text{ K min}^{-1}$ . (a)  $\text{NiCl}_2$ , (b)  $\text{ZnCl}_2$  and (c)  $\text{CdCl}_2$ .

perature when increasing the ion concentration, in agreement with the DSC results. For  $\text{Cd}^{2+}$  and  $\text{Zn}^{2+}$  a marked decrease in absorbance is observed at high temperatures ( $>60^\circ\text{C}$ ) for the highest ion concentrations, indicating probably a strong aggregation/precipitation of the samples in these conditions. At low concentration the melting curves of DNA in the presence of metal ions do not show significant differences (Fig. 6) and preserve the main characteristics showed by the DNA denaturation in the absence of metals.

Fig. 7 shows the curves obtained at the highest metal ion concentration, i.e.,  $0.0025 \text{ mol dm}^{-3}$ . The UV melting curves of DNA in the presence of  $\text{Zn}^{2+}$  and  $\text{Cd}^{2+}$  at this concentration differ significantly from the ones in the presence of  $\text{Mn}^{2+}$ ,  $\text{Co}^{2+}$  and  $\text{Ni}^{2+}$ , as



**Fig. 6.** Relative absorbance at 260 nm as a function of temperature for ds-DNA solutions with different metal ions. Citrate sodium buffer ( $[\text{NaCl}] = 7.5 \times 10^{-3} \text{ mol dm}^{-3}$ ),  $[c] = 0.0001 \text{ mol dm}^{-3}$ ,  $[\text{DNA}] = 0.05 \text{ mg cm}^{-3}$ ,  $\beta = 1 \text{ K min}^{-1}$ .

referred to above. In general, the profiles present two peaks for the denaturation of the DNA. In this figure, the profiles for  $\text{Cu}^{2+}$  are not included due to their stronger interaction and precipitation at this concentration.  $\text{Mn}^{2+}$ ,  $\text{Co}^{2+}$  and  $\text{Ni}^{2+}$  present a first peak of denaturation between 68 and 72 °C and the second peak between 76 and 80 °C. Generally speaking, the UV results are in accordance with the DSC ones, although some peaks observed in the DSC tracing cannot be detected by UV. Further, the UV profiles did show signs of precipitation/aggregation at concentrations not detected by eye before the DSC experiments.

Some melting studies of interactions between divalent ions and genomic DNAs have been published in the past [53]. The authors explained that some kind of fragmentation of DNA occurs irreversibly at low ionic strength (0.02 M  $\text{Na}^+$ ), whereas this effect disappears at a high ionic strength (0.2 M  $\text{Na}^+$ ). The results observed in this current paper are in agreement with suggested Kozyavkin and Lyubchenko [53] showing that the melting process is irreversible.

According the DSC data, it is possible to classify the effects of these metals in two groups, as discussed above. On one side we have  $\text{Cd}^{2+}$  and  $\text{Zn}^{2+}$ , which effect was the most destabilizing, presenting a significant decrease of the melting temperature (Fig. 5). It is possible to include also  $\text{Cu}^{2+}$  in this group, as the effect seems to be similar, although even stronger (higher precipitation)—already at  $0.015 \text{ mol dm}^{-3}$  the DSC profile showed a denaturation process

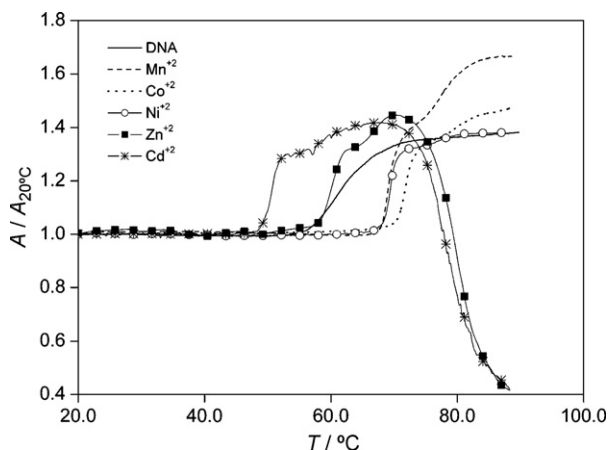


**Fig. 7.** Relative absorbance at 260 nm as a function of temperature for ds-DNA solutions with different metal ions. Citrate sodium buffer ( $[\text{NaCl}] = 7.5 \times 10^{-3} \text{ mol dm}^{-3}$ ),  $[c] = 0.0025 \text{ mol dm}^{-3}$ ,  $[\text{DNA}] = 0.05 \text{ mg cm}^{-3}$ ,  $\beta = 1 \text{ K min}^{-1}$ .

**Table 2**

UV thermal denaturation results. Citrate sodium buffer ( $[\text{NaCl}] = 7.5 \times 10^{-3} \text{ mol dm}^{-3}$ ,  $[\text{DNA}] = 0.05 \text{ mg cm}^{-3}$ ,  $\beta = 1 \text{ K min}^{-1}$ ).

Amostra	$c/\text{mol dm}^{-3}$	%H	$T_m/^\circ\text{C}$
DNA	0	38.7	60.7
$\text{Mn}^{2+}$	0.0001	39.8	65.6
	0.0005	40.8	70.7
	0.0010	36.8	74.6
	0.0025	*	69.2
$\text{Co}^{2+}$	0.0001	40.0	62.9
	0.0005	38.2	68.4
	0.0010	37.3	76.1
	0.0025	44.1	71.5
$\text{Ni}^{2+}$	0.0001	35.6	61.9
	0.0005	35.8	65.2
	0.0010	37.7	72.7
	0.0025	38.1	68.6
$\text{Cu}^{2+}$	0.0001	38.4	62.6
	0.0005	37.3	60.0
	0.00075	*	44.1
$\text{Zn}^{2+}$	0.0001	37.9	61.7
	0.0005	36.8	65.1
	0.0010	27.9	65.7
	0.0025	*	59.3
$\text{Cd}^{2+}$	0.0001	41.1	67.0
	0.0005	35.7	65.7
	0.0010	32.5	56.5
	0.0025	*	49.8

around 40 °C. On the other side we have the group formed by  $\text{Mn}^{2+}$ ,  $\text{Co}^{2+}$  and  $\text{Ni}^{2+}$ .

The hyperchomicity of the *Calf thymus* DNA was calculated in the absence and presence of the divalent metal ions at 260 nm. In their absence, it reaches a value of approximately 40% (Table 2). As can be seen in the table, the hyperchomicity values in the presence of these ions, does not change significantly with the increase in metal ion concentration.

#### 4. Conclusions

Interaction of calf thymus DNA with divalent metal was studied in a broad concentration range for different divalent cations. AS expected, DSC showed to be a very powerful technique for the following of DNA denaturation under different experimental conditions.

All ions investigated modify significantly the DSC melting profiles of ds-DNA. The changes are reflected in a shift of the temperatures of thermal denaturation, as well as in the shape of the DSC melting profiles (width, number and relative height of the peaks). The results obtained suggest a pronounced interaction of the metal ions with the base pairs, causing a decrease in the stability of the double helix. The enthalpy associated with  $\text{M}^{2+}$ -DNA formation shows significant dependence upon metal ion concentration.

For low concentration, there are no substantial modifications in thermal denaturation process of *Calf thymus* DNA in the absence and presence of divalent metal ion. Increasing metal ion concentration, there is a significant change of the thermal denaturation process.

The interaction of the  $\text{Cu}^{2+}$ ,  $\text{Cd}^{2+}$  and  $\text{Zn}^{2+}$  with the DNA bases is stronger than for  $\text{Mn}^{2+}$ ,  $\text{Co}^{2+}$  and  $\text{Ni}^{2+}$  showed destabilization of the ds-DNA.

These results obtained are in agreement with the general trends observed in the literature. Previous authors suggested that metal ions can bind to both the base and the phosphate and that all metal ions bind to the N7 atom of guanine. Based on our results, we can further suggest that  $\text{Ni}^{2+}$  binds also by chelation to the phosphate group (indicated by stabilization of the DNA). The interaction of the

$\text{Cu}^{2+}$  and  $\text{Cd}^{2+}$  with AT base was observed to destabilize the duplex helices.

In general the  $T_m$  values reported in Table 1 in the presence of cations are similar to or lower than those observed in their absence. It should be stressed, nevertheless, that the temperature reported is an “overall” temperature for the transition, although the occurrence of small peaks is evident from most tracings. Clearly at the highest ion concentrations, there is a significant decrease in the melting temperature, and the strength of this effect depends on metal ion. In general, any ligand that interacts more strongly with double-stranded than with single-stranded DNA will influence the thermodynamic parameters of helix-coil transition and hence also the DNA melting process by shifting the equilibrium toward stabilization of the helix form [41]. Consequently, low and moderate concentrations of metal cations may stabilize DNA and increase the melting temperature. The results reported in Table 2 are, thus, in good agreement with this state. As noted in the literature, this effect is restricted to very low metal concentrations. On the contrary, it has been reported that high concentrations of alkaline earths and transition metals cause rupture of hydrogen bonds, base unstacking, and, ultimately, decrease the thermal stability of DNA. The results obtained by DSC in the presence of the 20 times more concentrated metallic ions (Table 1) support this hypothesis.

Finally, the probable order of preference for base over phosphate for the metals studied has shown to be:  $\text{Cu}^{2+} > \text{Cd}^{2+} > \text{Zn}^{2+} > \text{Mn}^{2+} > \text{Co}^{2+} > \text{Ni}^{2+}$ .

## Acknowledgements

Thanks are due to *Fundação para a Ciência e Tecnologia (FCT)*, Lisbon, Portugal. H.K.S.S. thanks FCT and the European Social Fund (ESF) under the 3<sup>rd</sup> Community Support Framework (CSF) for the award of a Ph.D. research grant (SFRH/BD/11419/2002).

## References

- [1] R.M. Izatt, J.J. Christensen, J.H. Rytting, *Chem. Rev.* 71 (1971) 439–481.
- [2] I. Sissoëff, J. Grisvard, E. Guillé, *Prog. Biophys. Molec. Biol.* 31 (1978) 165–199.
- [3] E.V. Hackl, S.V. Kornilova, Y.P. Blagoi, *Int. J. Biol. Macromol.* 35 (2005) 175–191.
- [4] V.A. Sorokin, V.A. Valeev, G.O. Gladchenko, I.V. Sisa, Y.P. Blagoi, I.V. Volchok, *J. Inorg. Biochem.* 63 (1996) 79–98.
- [5] I. Rouzina, V.A. Bloomfield, *Biophys. J.* 74 (1998) 3152–3164.
- [6] D.O. Wood, M.J. Dinsmore, G.A. Bare, J.S. Lee, *Nucleic Acids Res.* 30 (2002) 2244–2250.
- [7] V.G. Vaidyanathan, B.U. Nair, *J. Inorg. Biochem.* 95 (2003) 334–342.
- [8] R. Vijayalakshmi, M. Kanthimathi, V. Subramanian, B.U. Nair, *Biochem. Biophys. Acta* 1475 (2000) 157–162.
- [9] Y.S. Tarahovsky, V.A. Rakhmanova, R.M. Epand, R.C. MacDonald, *Biophys. J.* 82 (2002) 264–273.
- [10] H.-A. Tajmir-Riahi, M. Naoui, R. Ahmad, *Biopolymers* 33 (1993) 1819–1827.
- [11] P.R. Reddy, M. Radhika, K.S. Rao, *J. Chem. Sci.* 116 (2004) 221–226.
- [12] Z. Wang, Z. Zhang, D. Liu, S. Dong, *Spectrochim. Acta Part A* 59 (2003) 949–956.
- [13] G.M. Merlishvili, M.J. Sottomayor, M.A.V. Ribeiro da Silva, T.D. Mdzinarashvili, M. Al-Zaza, M. Tediashvili, D. Tushshvili, N. Chanishvili, *J. Therm. Anal. Calc.* 66 (2001) 103–113.
- [14] V.A. Sorokin, V.A. Valeev, G.O. Gladchenko, M.V. Degtyar, E.A. Andrus, V.A. Karachetvsev, Y.P. Blagoi, *Int. J. Biol. Macromol.* 35 (2005) 201–210.
- [15] P. Wu, Y. Kawamoto, H. Hara, N. Sugimoto, *J. Inorg. Biochem.* 91 (2002) 277–285.
- [16] L. Petraccone, S. Baiano, G. Fiorentino, G. Barone, C. Giancola, *Thermochim. Acta* 418 (2004) 47–52.
- [17] M. Asadi, E. Safaei, B. Ranjbar, L. Hasani, *New J. Chem.* 28 (2004) 1227–1234.
- [18] A. Bouskila, E. Amouyal, C. Verchere-Bear, I. Sasaki, A. Gaudemer, *J. Photochem. Photobiol.*, B 76 (2004) 69–83.
- [19] D.H. Tjahjono, S. Mima, T. Akutsu, N. Yoshioka, H. Inoue, *J. Inorg. Biochem.* 85 (2001) 219–228.
- [20] A. Hormann, B. Chaudhuri, H. Fretz, *Bioorg. Med. Chem.* 9 (2001) 917–921.
- [21] P.D. Vecchio, D. Esposito, L. Ricchi, G. Barone, *Int. J. Biol. Macromol.* 24 (1999) 361–369.
- [22] S.C.M. Gandini, I.E. Borissevitch, J.R. Perussi, H. Imasato, M. Tabak, *J. Lumin.* 78 (1998) 53–61.
- [23] E. Suleymanoglu, *Il Farmaco* 60 (2005) 701–710.
- [24] B.G. Moreira, Y. You, M.A. Behlke, R. Owczarzy, *Biochem. Biophys. Commun.* 327 (2005) 473–484.
- [25] M. Tabata, A.K. Sarker, E. Nyarko, *J. Inorg. Biochem.* 94 (2003) 50–58.
- [26] G. Barone, F. Catanzano, P.D. Vecchio, C. Giancola, G. Graziano, *Pure Appl. Chem.* 69 (1997) 2307–2313.
- [27] D. Esposito, P. Del Vecchio, G. Barone, *J. Am. Chem. Soc.* 119 (1997) 2606–2613.
- [28] J.G. Duguid, V.A. Bloomfield, J.M. Benevides, G.J. Thomas Jr., *Biophys. J.* 69 (1995) 2623–2641.
- [29] D. Beyersmann, *Toxicol. Lett.* 72 (1994) 333–338.
- [30] D.W. Gruenwedel, *Biochim. Biophys. Acta* 340 (1974) 16–30.
- [31] E. Suleymanoglu, *Rev. Electron. Biomed./Electron. J. Biomed.* 2 (2004) 13–35.
- [32] L. Petraccone, E. Erra, A. Mesere, D. Montesarchio, G. Piccialli, G. Barone, C. Giancola, *Biophys. Chem.* 104 (2003) 259–270.
- [33] R. Owczarzy, *Thermochim. Acta* 373 (2001) 153–160.
- [34] I. Jelesarov, H.R. Bosshard, *J. Mol. Recogn.* 12 (1999) 3–18.
- [35] M.C. Chakrabarti, F.P. Schwarz, *Nucleic Acids Res.* 27 (1999) 4801–4806.
- [36] J.G. Duguid, V.A. Bloomfield, J.M. Benevides, G.J. Thomas Jr., *Biophys. J.* 71 (1996) 3350–3360.
- [37] B.S. McCrary, S.P. Edmondson, J.W. Shriver, *J. Mol. Biol.* 264 (1996) 784–805.
- [38] A.E. Beezer, *Biological Microcalorimetry*, Academic Press, London, 1980.
- [39] R.M. Wartell, A.S. Benight, *Phys. Rep.* 126 (1985) 67–107.
- [40] L.A. Marky, K.J. Breslauer, *Biopolymers* 26 (1987) 1601–1620.
- [41] V. Bloomfield, D.M. Crothers, I.T. Jr., *Nucleic Acids—Structures, Properties and Functions.*, California, University Science Books, 2000.
- [42] A. Schöppe, H. Hinz, H. Rosemeyer, F. Seela, *Eur. J. Biochem.* 239 (1996) 33–41.
- [43] G.M. Mervlishvili, M.J. Sottomayor, M.A.V. Ribeiro da Silva, *Thermochim. Acta* 394 (2002) 83–88.
- [44] F.E. Rossetto, E. Nieboer, *J. Inorg. Biochem.* 54 (1994) 167–186.
- [45] D.T. Browne, J. Eisinger, N.J. Leonard, *J. Am. Chem. Soc.* 90 (1968) 7302–7323.
- [46] V. Ostadná, N. Dolinnaya, S. Andreev, T. Oretskaya, J. Wang, T. Hianik, *Bioelectrochem* 67 (2005) 205–210.
- [47] I. Rouzina, V.A. Bloomfield, *Biophys. J.* 77 (1999) 3252–3255.
- [48] E.V. Hackl, Y.P. Blagoi, *J. Inorg. Biochem.* 98 (2004) 1911–1920.
- [49] V. Bregadze, I. Khutsishvili, J. Chkaberidze, K. Sologhashvili, *Inorg. Chim. Acta* 339 (2002) 145.
- [50] C. Hofr, V. Brabec, *Biopolymers* 77 (2005) 222–229.
- [51] S.D. Wettig, D.O. Wood, J.S. Lee, *J. Inorg. Biochem.* 94 (2003) 94–99.
- [52] G.L. Eichhorn, Y.A. Shin, *J. Am. Chem. Soc.* 90 (1968) 7323–7328.
- [53] S.A. Kozyavkin, Y.L. Lyubchenko, *Nucleic Acids Res.* 12 (1984) 4339–4349.